

QCD condensates and α_s from τ -decay

Stephan Narison

*Laboratoire Univers et Particules de Montpellier (LUPM), CNRS-IN2P3,
Case 070, Place Eugène Bataillon, 34095 - Montpellier, France*

and

*Institute of High-Energy Physics of Madagascar (iHEPMAD)
University of Ankatso, Antananarivo 101, Madagascar*

Abstract

We improve the determinations of the QCD condensates within the SVZ expansion in the axial-vector (A) channel using the ratio of Laplace sum rule (LSR) $\mathcal{R}_{10}^A(\tau)$ within stability criteria and τ -like higher moments $\mathcal{R}_{n,A}$ within stability for arbitrary τ -mass squared s_0 . We find the same violation of the factorization by a factor 6 of the four-quark condensate as from $e^+e^- \rightarrow \text{Hadrons}$ data. One can notice a systematic alternate sign and no exponential growth of the size of these condensates. Then, we extract α_s from the lowest τ -decay like moment. We obtain to order α_s^4 the conservative value from the s_0 -stability until M_τ^2 : $\alpha_s(M_\tau)|_A = 0.3178(66)$ (FO) and $0.3380(44)$ (CI) leading to: $\alpha_s(M_Z)|_A = 0.1182(8)_{fit(3)evol.}$ (FO) and $0.1206(5)_{fit(3)evol.}$ (CI). We extend the analysis to the channel and find: $\alpha_s(M_\tau)|_{V-A} = 0.3135(83)$ (FO) and $0.3322(81)$ (CI) leading to: $\alpha_s(M_Z)|_{V-A} = 0.1177(10)_{fit(3)evol.}$ (FO) and $0.1200(9)_{fit(3)evol.}$ (CI). We observe that in different channels ($e^+e^- \rightarrow \text{Hadrons}$, A, V, V-A), the extraction of $\alpha_s(M_\tau)$ at the observed τ -mass leads to an overestimate of its value. Our determinations from these different channels lead to the mean: $\alpha_s(M_\tau) = 0.3140(44)$ (FO) and $0.3346(35)$ (CI) leading to: $\alpha_s(M_Z) = 0.1178(6)_{fit(3)evol.}$ (FO) and $0.1202(4)_{fit(3)evol.}$ (CI). Comparisons with some other results are done.

Keywords: QCD spectral sum rules, QCD condensates, α_s , τ -decay, $e^+e^- \rightarrow \text{Hadrons}$.

Email address: snarison@yahoo.fr (Stephan Narison)

1. Introduction

In this paper, we pursue the determinations of the QCD condensates and α_s done in [1, 2] for the $e^+e^- \rightarrow$ Hadrons and the vector (V) current to the case of axial-vector (A) and V-A currents. In so doing, we shall use the τ sum rule variable stability criteria for the Laplace sum rule and the M_τ stability for the τ -like moment sum rule.

Definitions and normalizations of observables will be the same as in Ref. [1, 2] and will not be extensively discussed here.

2. The axial-vector (A) two-point function

• The two-point function

We shall be concerned with the two-point correlator :

$$\begin{aligned}\Pi_{V(A)}^{\mu\nu}(q^2) &= i \int d^4x e^{-iqx} \langle 0 | \mathcal{T} J_{V(A)}^\mu(x) \left(J_{V(A)}^\nu(0) \right)^\dagger | 0 \rangle \\ &= -(g^{\mu\nu} q^2 - q^\mu q^\nu) \Pi_{V(A)}^{(1)}(q^2) + q^\mu q^\nu \Pi_{V(A)}^{(0)}(q^2)\end{aligned}\quad (1)$$

built from the T-product of the bilinear axial-vector current of u, d quark fields:

$$J_{V(A)}^\mu(x) =: \bar{\psi}_u \gamma^\mu (\gamma_5) \psi_d :. \quad (2)$$

The upper indices (0) and (1) correspond to the spin of the associated hadrons. The two-point function obeys the dispersion relation:

$$\Pi_{V(A)}(q^2) = \int_{t>}^\infty \frac{dt}{t - q^2 - i\epsilon} \frac{1}{\pi} \text{Im} \Pi_{V(A)}(t) + \dots, \quad (3)$$

where \dots are subtraction constants polynomial in q^2 and $t >$ is the hadronic threshold.

• QCD expression of the two-point function

Within the SVZ-expansion [3], the two-point function can be expressed in terms of the sum of higher and higher quark and gluon condensates:

$$4\pi^2 \Pi_H(-Q^2, m_q^2, \mu) = \sum_{D=0,2,4,\dots} \frac{C_{D,H}(Q^2, m_q^2, \mu) \langle O_{D,H}(\mu) \rangle}{(Q^2)^{D/2}} \equiv \sum_{D=0,2,4,\dots} \frac{d_{D,H}}{(Q^2)^{D/2}}, \quad (4)$$

where $H \equiv V(A)$, μ is the subtraction scale which separates the long (condensates) and short (Wilson coefficients) distance dynamics and m_q is the quark mass.

◊ In the chiral limit [4, 5]:

$$\begin{aligned}d_{2,A} &= d_{2,V} = 0, \\ d_{4,A} &= d_{4,V} = \frac{\pi}{3} \langle \alpha_s G^2 \rangle \left(1 + \frac{7}{6} a_s \right), \\ d_{6,A} &= - \left(\frac{11}{7} \right) d_{6,V} = \frac{1408}{81} \pi^3 \rho \alpha_s \langle \bar{\psi} \psi \rangle^2, \\ d_{8,A} &\approx d_{8,V} \approx - \frac{39}{162} \pi \langle \alpha_s G^2 \rangle^2\end{aligned}\quad (5)$$

where ρ measures the deviation from the factorization of the 4-quark condensates and the last equality for d_8 is based on vacuum saturation estimate of some classes of computed dimension-8 diagrams.

◊ The perturbative expression of the spectral function is known to order α_s^4 [6, 7]. It reads for 3 flavours:

$$4\pi \text{Im}\Pi_H(t) = 1 + a_s + 1.6398a_s^2 - 10.2839a_s^3 - 106.8798a_s^4 + \mathcal{O}(a_s^5), \quad (6)$$

where :

$$a_s \equiv \frac{\alpha_s}{\pi} = \frac{2}{-\beta_1 \text{Log}(t/\Lambda^2)} + \dots, \quad (7)$$

where $-\beta_1 = (1/2)(11 - 2n_f/3)$ is the first coefficient of the β -function and n_f is the number of quark flavours; \dots stands for higher order terms which can e.g. be found in [8]. We shall use the value $\Lambda = (342 \pm 8)$ MeV for $n_f = 3$ from the PDG average [9].

- *Spectral function from the data*

We shall use the recent ALEPH data [10] in Fig. 1 for the spectral function $a_1(s)$.

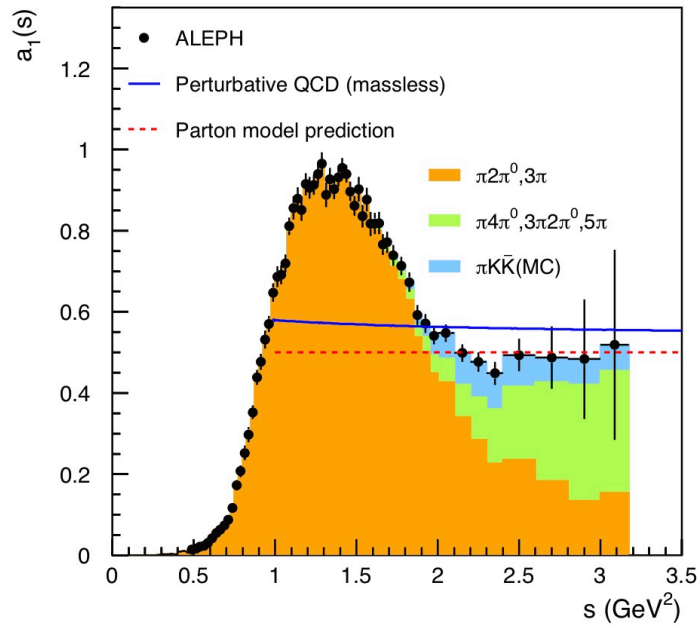


Figure 1: ALEPH data of the axial-vector spectral function.

Like in the case of the vector spectral function from $e^+e^- \rightarrow \text{Hadrons}$ [2], we subdivide the region from 3π threshold to $M_\tau^2 = 3.16 \text{ GeV}^2$ into different subregions in s (units in $[\text{GeV}^2]$):

$$s = [0.4, 0.8], [0.8, 1.29], [1.29, 1.42], [1.42, 2.35], [2.35, 3.16], \quad (8)$$

and fit the data with 3rd order polynomials using the optimized Mathematica program FindFit except for $[1.29, 1.42]$ where a 2nd order polynomial is used. We show the different fits in the Fig. 2.

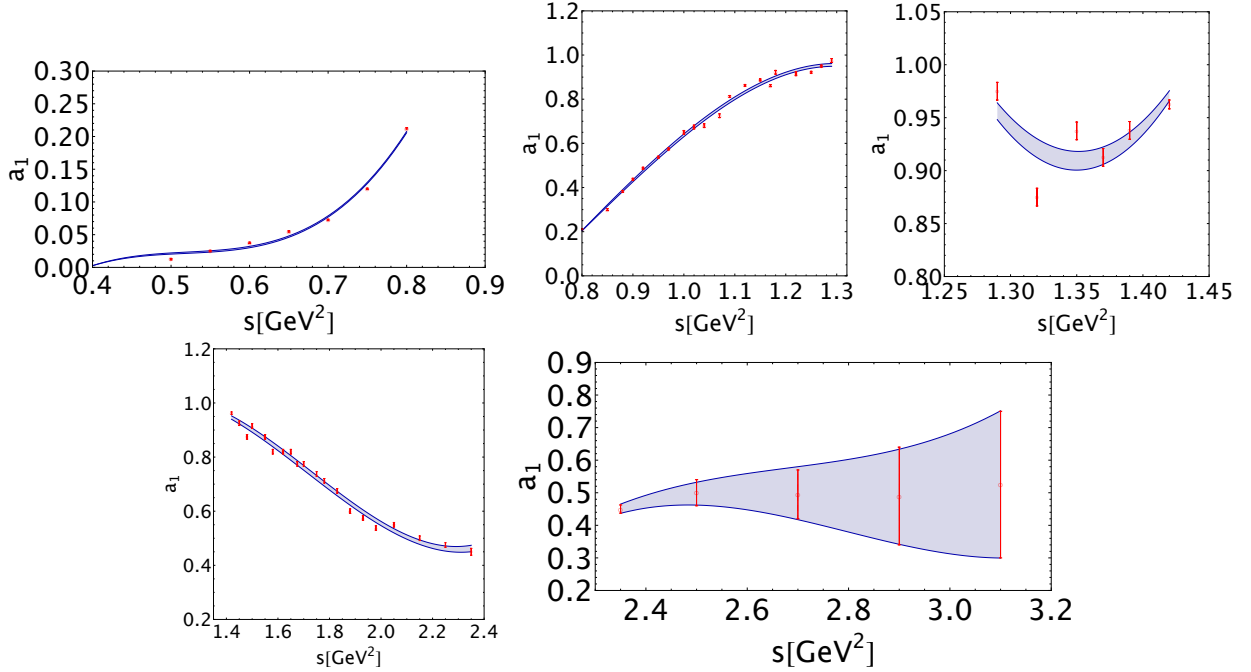


Figure 2: Fit of the data using a 2nd and 3rd order polynomial fits.

3. The ratio of Laplace sum rule (LSR) moments

Like in the case of vector channel, we shall use here the ratio of LSR moments [3, 11, 12]¹:

$$\mathcal{R}_{10}^A(\tau) \equiv \frac{\mathcal{L}_1^c}{\mathcal{L}_0^c} = \frac{\int_{t>}^{t_c} dt e^{-t\tau} t \frac{1}{\pi} \text{Im}\Pi_H(t, \mu^2, m_q^2)}{\int_{t>}^{t_c} dt e^{-t\tau} \frac{1}{\pi} \text{Im}\Pi_H(t, \mu^2, m_q^2)}, \quad (9)$$

where τ is the LSR variable, $t >$ is the hadronic threshold. Here t_c is the threshold of the “QCD continuum” which parametrizes, from the discontinuity of the Feynman diagrams, the spectral function $\text{Im}\Pi_H(t, m_q^2, \mu^2)$. m_q is the quark mass and μ is an arbitrary subtraction point.

• QCD expression of the LSR moments

To order α_s^4 , the perturbative (PT) expression of the lowest moment reads [1]:

$$\mathcal{L}_0^{PT}(\tau) = \frac{3}{2}\tau^{-1} \left[1 + a_s + 2.93856 a_s^2 + 6.2985 a_s^3 + 22.2233 a_s^4 \right]. \quad (10)$$

Then, taking its derivative in τ , one gets $\mathcal{L}_1(\tau)$ and then their ratio $\mathcal{R}_{10}(\tau)$.

From Eq. 4, one can deduce the non-perturbative contribution to the lowest LSR moment :

$$\mathcal{L}_0^{NPT}(\tau) = \frac{3}{2}\tau^{-1} \sum_D \frac{d_D}{(D/2 - 1)!} \tau^{D/2}, \quad (11)$$

from which one can deduce \mathcal{L}_1^{NPT} and \mathcal{R}_{10}^A .

¹For a recent review, see e.g. [13].

- $d_{6,A}$ and $d_{8,A}$ from \mathcal{R}_{10}^A

We show in Fig. 3a) the τ behaviour of the phenomenological side of \mathcal{R}_{10}^A (experiment \oplus QCD continuum beyond the threshold t_c) for values of t_c around the physical τ -lepton mass squared where the effect of t_c is negligible.

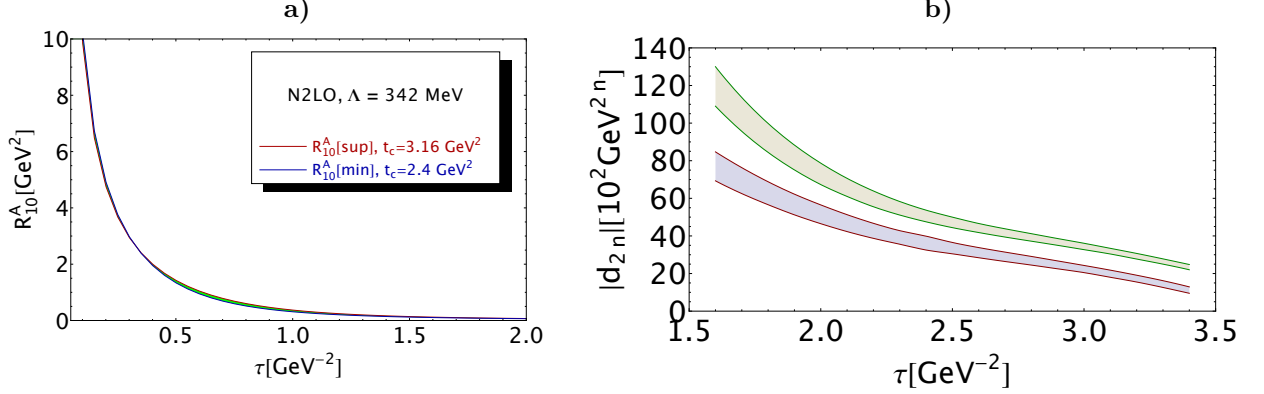


Figure 3: a): R_{10}^A versus the LSR variable τ ; b): $d_{6,A}$ and $d_{8,A}$ from the \mathcal{R}_{10}^A

For determining $d_{6,A}$ and $d_{8,A}$, we use as input the more precise value of $\langle \alpha_s G^2 \rangle$ from the heavy quark mass-splittings and some other sum rules [14, 15]:

$$\langle \alpha_s G^2 \rangle = (6.39 \pm 0.35) \times 10^{-2} \text{ GeV}^4, \quad (12)$$

and perform a two-parameter fit ($d_{6,A}, d_{8,A}$) by confronting the phenomenological and QCD side of R_{10}^A for different values of τ . The QCD coupling α_s is evaluated at the LSR sum rule scale τ where we use $\Lambda = (342 \pm 8) \text{ MeV}$ for $n_f = 3$ flavours deduced from the PDG world average [9]. The results of the analysis are shown in Fig. 3. There is an inflexion point around $\tau \simeq 2.5 \text{ GeV}^{-2}$ at which we extract the optimal values of the condensates. One should note that at this scale the OPE converges quite well in the vector channel [1]. Then, we may expect that for the axial-vector the same feature occurs. We obtain the optimal result:

$$d_{6,A} = (33.5 \pm 3.0 \pm 2.7) \times 10^{-2} \text{ GeV}^6 \quad d_{8,A} = -(47.2 \pm 2.8 \pm 3.2) \times 10^{-2} \text{ GeV}^8 \quad (13)$$

where the 1st error comes from the fitting procedure and the 2nd one from the localization of $\tau \simeq (2.5 \pm 0.1) \text{ GeV}^{-2}$.

- $\langle \alpha_s G^2 \rangle$ from \mathcal{R}_{10}^A

We use the previous values of $d_{6,A}$ and $d_{8,A}$ into \mathcal{R}_{10}^A and we re-extract $\langle \alpha_s G^2 \rangle$ using a one-parameter fit. The analysis is shown in Fig. 4. We obtain:

$$\langle \alpha_s G^2 \rangle = (6.9 \pm 1.5) \times 10^{-2} \text{ GeV}^4, \quad (14)$$

in good agreement with the one in Eq. 12 used previously as input. This result also indicates the self-consistency of the set of condensates entering in the analysis.

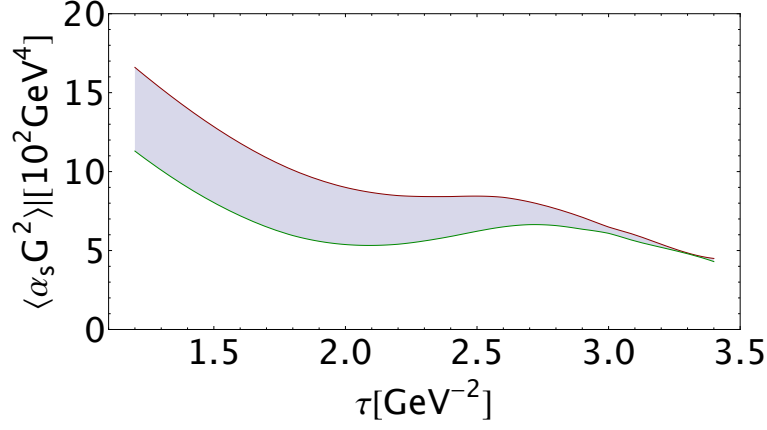


Figure 4: $\langle \alpha_s G^2 \rangle$ versus the LSR variable τ .

4. BNP τ -decay like moments

As emphasized by BNP in Ref. [4, 5], it is more convenient to express the moment in terms of the combination of Spin (1+0) and Spin 0 spectral functions in order to avoid some eventual pole from $\Pi^{(0)}$ at $s = 0$:

$$\mathcal{R}_{n,H} = 6\pi i \int_{|s|=M_0^2} dx (1-x)^2 x^n \left((1+2x) \Pi_H^{(1+0)}(x) - 2x \Pi_H^{(0)}(x) \right) \quad (15)$$

with $x \equiv s/M_0^2$, $H \equiv V, A$. n indicates the degree of moment. The lowest moment $\mathcal{R}_{0,A}$ corresponds to the physical τ -decay process [4, 5].

- The lowest moment $\mathcal{R}_{0,A}$ from the data

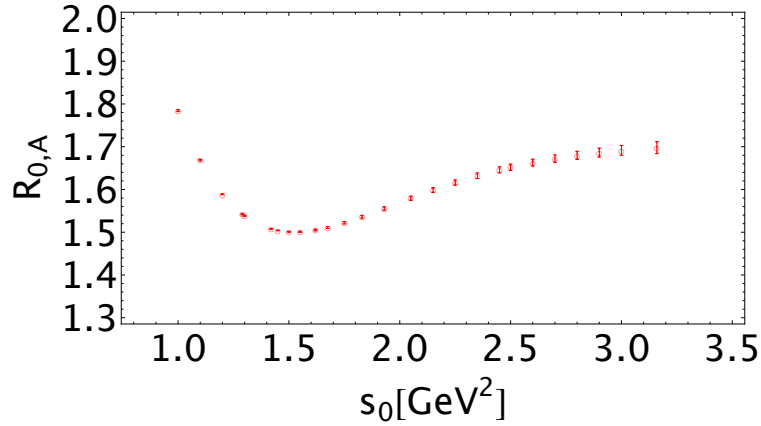


Figure 5: Lowest moment $\mathcal{R}_{0,A}$ versus the hypothetical τ -mass squared s_0 .

Using previous fits of the data, we show in Fig. 5 the behaviour of the lowest moment $\mathcal{R}_{0/A}$ versus an hypothetical τ -lepton mass squared $s_0 \equiv M_0^2$. At the observed mass value: $M_\tau = 1.777$ GeV, one obtains:

$$\mathcal{R}_{0,A} = 1.698(14). \quad (16)$$

It reproduces with high accuracy the ALEPH value [10] :

$$\mathcal{R}_{0,A}|_{\text{Aleph}} = 1.694(10), \quad (17)$$

which is an important self-consistency test of our fitting procedure.

- *The lowest BNP moment $\mathcal{R}_{0,A}$*

The QCD expression of $\mathcal{R}_{0,A}$ including the dimension six ($d_{6,A}$) and eight ($d_{8,A}$) condensates within the SVZ expansion [3] can be deduced from [4]. To simplify for the reader, we give its expression, in the chiral limit ²:

$$\mathcal{R}_{0,A} = \frac{N_c}{2} |V_{ud}|^2 S_{ew} \left\{ 1 + \delta'_{ew} + \delta_A^{(0)} + \sum_{D=1,2,\dots} \delta_A^{(2D)} \right\}. \quad (18)$$

where the electroweak factors and corrections are :

$$V_{ud} = 0.97418, \quad S_{ew} = 1.019, \quad \delta'_{ew} = 0.0010. \quad (19)$$

The QCD corrections copied from BNP are:

◊ Perturbative corrections to order α_s^4 :

$$\begin{aligned} \delta_A^{(0)}|_{FO} &= a_s + 5.2023 a_s^2 + 26.366 a_s^3 + 127.079 a_s^4, \\ \delta_A^{(0)}|_{CI} &= 1.364 a_s + 2.54 a_s^2 + 9.71 a_s^3 + 64.29 a_s^4, \end{aligned} \quad (20)$$

for fixed order (FO) [4] and contour improved (CI) [16].

Observing that the PT series grows geometrically [17] from the calculated coefficients in different channels, we estimate the a_s^5 coefficient to be [1] :

$$\delta_5^{FO} \approx \pm 552 a_s^5, \quad \delta_5^{CI} \approx \pm 228 a_s^5, \quad (21)$$

which one can consider either to be the error due to the unknown higher order terms of the series or (more optimistically) to be the estimate of the uncalculated α_s^5 coefficient.

◊ Power corrections up to $d_{8,A}$:

They read:

$$\begin{aligned} \delta_A^{(2)} &= -8 \left(1 + \frac{16}{3} a_s \right) \frac{(m_u^2 + m_d^2)}{M_0^2} - 4 \left(1 + \frac{25}{3} a_s \right) \frac{(m_u m_d)}{M_0^2}, & \delta_A^{(2)}|_{tach} &= -2 \times 1.05 \frac{a_s \lambda^2}{M_0^2}, \\ \delta_A^{(4)} &= \frac{11\pi}{4} a_s^2 \frac{\langle \alpha_s G^2 \rangle}{M_0^4} + 32\pi^2 \left(1 + \frac{63}{16} a_s^2 \right) \frac{(m_u + m_d) \langle \bar{\psi}_u \psi_u \rangle}{M_0^4} - 8\pi^2 \sum_k \frac{m_k \langle \bar{\psi}_k \psi_k \rangle}{M_0^4} + \mathcal{O}(m_q^4) \\ \delta_A^{(6)} &= -6 \frac{d_{6,A}}{M_0^6}, & \delta_A^{(8)} &= -4 \frac{d_{8,A}}{M_0^8}, \end{aligned} \quad (22)$$

where $s_0 \equiv M_0^2$ while $d_{6,A}$ and $d_{8,A}$ have been defined in Eqs. 5 . We have assumed $\langle \bar{\psi}_u \psi_u \rangle = \langle \bar{\psi}_d \psi_d \rangle$. We shall not include the $D = 2$ contribution due to an eventual tachyonic gluon mass within the standard OPE.

²We use the complete expression including quark masses and α_s corrections in the numerical analysis.

Using duality [17], this term can be included in the estimate of the non-calculated higher order terms of the PT series discussed previously. Instanton contributions are expected to have higher dimensions and their contributions can be safely neglected [1].

- $d_{6,A}$ and $d_{8,A}$ condensates from $\mathcal{R}_{0,A}$

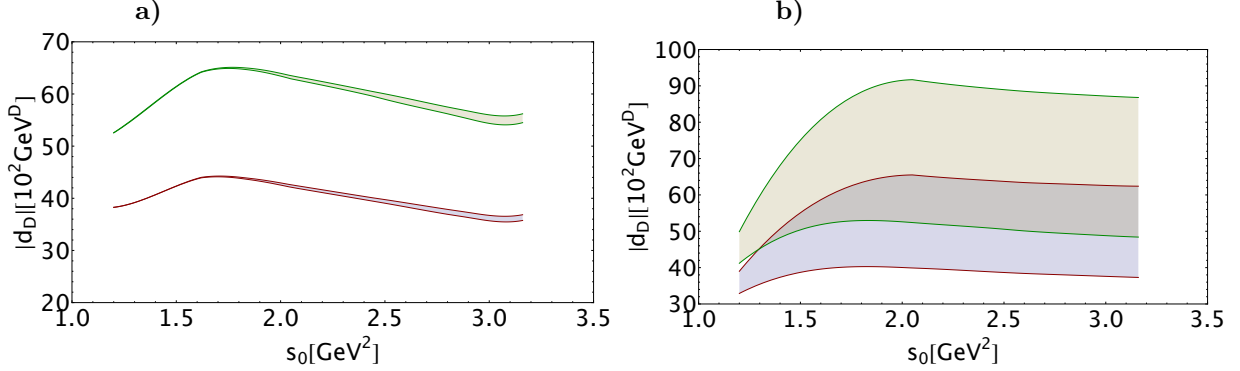


Figure 6: **a)**: $|d_{6,A}|$ (lowest curve) and $|d_{8,A}|$ (highest curve) versus M_0^2 ; **b)**: similar to **a)** but for $|d_{8,A}|$ and $|d_{10,A}|$.

We confront the experimental and QCD sides of $\mathcal{R}_{0,A}$ for different values of s_0 . Like in the case of the ratio of Laplace sum rules, we use a two-parameter fit $(d_{6,A}, d_{8,A})$ to extract the values of these condensates using as input the values of the d_4 condensates and light quark masses. We consider the PT series up to order α_s^4 and evaluate α_s at the hypothetical τ -mass squared $s_0 = M_0^2$. We use $\Lambda = (342 \pm 8) \text{ MeV}$ for $n_f = 3$ flavours from the PDG world average [9]. The results versus s_0 are shown in Fig. 6a).

We consider as a reliable value the one from $s_0 = 1.93 \text{ GeV}^2$ beyond the peak of the A_1 meson. We notice a stability (minimum) around 3 GeV^2 just below the physical τ mass which we consider as our optimal value:

$$\begin{aligned} d_{6,A} &= (36.2 \pm 0.5) \times 10^{-2} \text{ GeV}^6 & d_{8,A} &= -(55.2 \pm 0.9) \times 10^{-2} \text{ GeV}^8 & (\text{FO}) \\ d_{6,A} &= (33.1 \pm 0.5) \times 10^{-2} \text{ GeV}^6 & d_{8,A} &= -(50.6 \pm 0.8) \times 10^{-2} \text{ GeV}^8 & (\text{CI}) \end{aligned} \quad (23)$$

One can notice from the analysis that the absolute values of the condensates are slightly higher for FO than for CI. To be conservative, we take the arithmetic average of the FO and CI values and add as a systematic the largest distance between the mean and the individual value:

$$d_{6,A} = (34.6 \pm 1.8) \times 10^{-2} \text{ GeV}^6 \quad d_{8,A} = -(52.9 \pm 2.4) \times 10^{-2} \text{ GeV}^8. \quad (24)$$

5. $d_{8,A}$ and $d_{10,A}$ from $\mathcal{R}_{1,A}$

The expression of $\mathcal{R}_{1,A}$ is similar to $\mathcal{R}_{1,V}$ given in Eq. 20 of Ref. [1]. Using a two-parameter fit $(d_{8,A}, d_{10,A})$ of $\mathcal{R}_{1,A}$ for different s_0 , we show the result of the analysis in Fig. 6b) using FO PT series. One obtains:

$$d_{8,A} = -(51.4 \pm 11.0) \times 10^{-2} \text{ GeV}^6 \quad d_{10,A} = (70.1 \pm 21.6) \times 10^{-2} \text{ GeV}^8. \quad (25)$$

The results are stable versus s_0 but less accurate than in the case of $\mathcal{R}_{0,A}$ such that one cannot differentiate a FO from CI truncation of the PT series. Then, for higher moments, we shall only consider FO PT series.

6. Final values of $d_{6,A}$ and $d_{8,A}$

As a final value of $d_{6,A}$, we take the mean of the values in Eqs. 13 and 24. We obtain:

$$d_{6,A} = (34.4 \pm 1.7) \times 10^{-2} \text{ GeV}^6, \quad (26)$$

while for $d_{8,A}$, we take the mean of the values obtained in Eqs. 13, 24 and 25. We obtain:

$$d_{8,A} = -(51.51 \pm 2.08) \times 10^{-2} \text{ GeV}^8. \quad (27)$$

◊ We notice that the relation :

$$d_{6,A} \simeq -(11/7) d_{6,V}, \quad (28)$$

is quite well satisfied within the errors. This result also suggests a violation of the four-quark condensate vacuum saturation (see Eq. 5) similar to the one found from $e^+e^- \rightarrow \text{Hadrons}$ data [1, 2]:

$$\rho \alpha_s \langle \bar{\psi}\psi \rangle^2 = (6.38 \pm 0.30) \times 10^{-4} \text{ GeV}^6 \quad \longrightarrow \quad \rho \simeq (6.38 \pm 0.30). \quad (29)$$

• Determination of $\alpha_s(M_\tau)$

We use the previous values of $d_{6,A}$ and $d_{8,A}$ together with the one of $\langle \alpha_s G^2 \rangle$ in Eq.12 as inputs in the lowest BNP moment $\mathcal{R}_{0,A}$ in order to determine $\alpha_s(M_\tau)$. We show in Fig. 7, the behaviour of $\alpha_s(M_\tau)$ versus an hypothetical τ mass squared $M_0^2 \equiv s_0$. One can notice an inflexion point in the region $2.5_{-0.15}^{+0.10} \text{ GeV}^2$ at which we extract the optimal result. The conservative result from $s_0 = 2.1 \text{ GeV}^2$ to M_τ^2 (see Fig. 7) is:

$$\begin{aligned} \alpha_s(M_\tau)|_A &= 0.3178(10)(65) & \longrightarrow & \alpha_s(M_Z)|_A = 0.1182(8)(3)_{evol} & \text{(FO)} \\ &= 0.3380(10)(43) & \longrightarrow & \alpha_s(M_Z)|_A = 0.1206(5)(3)_{evol} & \text{(CI).} \end{aligned} \quad (30)$$

The 1st error in $\alpha_s(M_\tau)|_A$ comes from the fitting procedure. The 2nd one comes from an estimate of the α_s^5 contribution from Ref. [1]. At the scale $s_0 = 2.5 \text{ GeV}^2$ the sum of non-perturbative contributions to the moment normalized to the parton model is:

$$\delta_{NP,A} \simeq -(7.9 \pm 1.1) \times 10^{-2}. \quad (31)$$

One can notice that extracting $\alpha_s(M_\tau)|_A$ at the observed τ -mass tends to overestimate the result:

$$\alpha_s(M_\tau)|_A = 0.3352(40) \quad \text{FO}, \quad 0.3592(47) \quad \text{CI.} \quad (32)$$

These values extracted at M_τ agree with the ones from Ref. [18] obtained at the same scale. The same feature has been observed in the case of $e^+e^- \rightarrow \text{Hadrons}$.

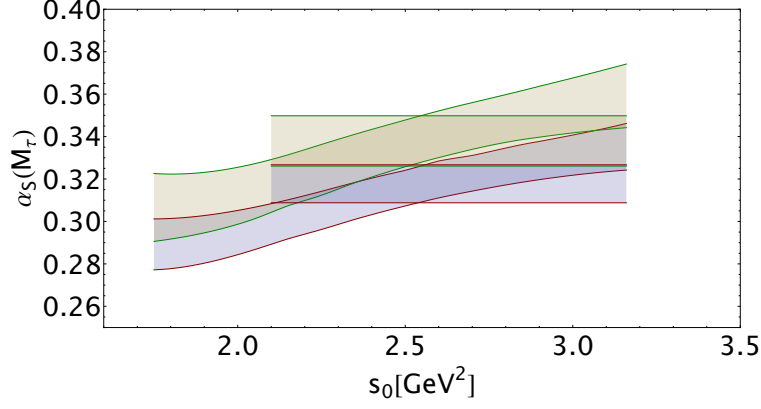


Figure 7: $\alpha_s(M_\tau)$ versus the hypothetical τ -mass squared s_0 .

Channel	d_6	$-d_8$	$\alpha_s(M_\tau)$ FO	$\alpha_s(M_\tau)$ CI	Refs.
e^+e^-	$-(26.3 \pm 3.7)$	$-(18.2 \pm 0.6)$	0.3081(86)	0.3260(78)	[1]
V			0.3129(79)	0.3291(70)	[1]
A	34.4 ± 1.7	51.5 ± 2.1	0.3157(65)	0.3368(45)	This work
A	43.4 ± 13.8	59.2 ± 19.7	0.3390(180)	0.3640(230)	[18]
A	19.7 ± 1.0	27 ± 1.2	—	0.3350(120)	[10]
A	9.6 ± 3.3	9.0 ± 5.0	0.3230(160)	0.3470(230)	[20]

Table 1: Values of the QCD condensates from some other τ -moments at Fixed Order (FO) PT series and of $\alpha_s(M_\tau)$ for FO and Contour Improved (CI) PT series.

• Comparison with previous results

We compare our results with the ones from e^+e^- and τ -decay Vector channel [1] and with the results obtained by different authors in the Axial-Vector channel:

◊ Our values of $d_{6,A}$ and $d_{8,A}$ are in good agreement within the errors with the ones of Ref. [18] but about two times larger than the ones of Ref. [10].

◊ The value of $d_{8,A}$ suggests that the assumption in Eq. 5:

$$d_{8,A} \approx d_{8,V} \quad (33)$$

is not satisfied by the fitted values given in Table 1.

7. High-dimension condensates

To determine the high-dimension condensates, we use the analogue of the moments given Eq. 19 of Ref. [1] for the vector channel.

- $d_{10,A}$ and $d_{12,A}$ condensates from $\mathcal{R}_{2,A}$

We use a two-parameter fit to extract $(d_{10,A}, d_{12,A})$ from $\mathcal{R}_{2,A}$, $(d_{12,A}, d_{14,A})$ from $\mathcal{R}_{3,A}$. The s_0 behaviour of the results is given in Fig. 8.

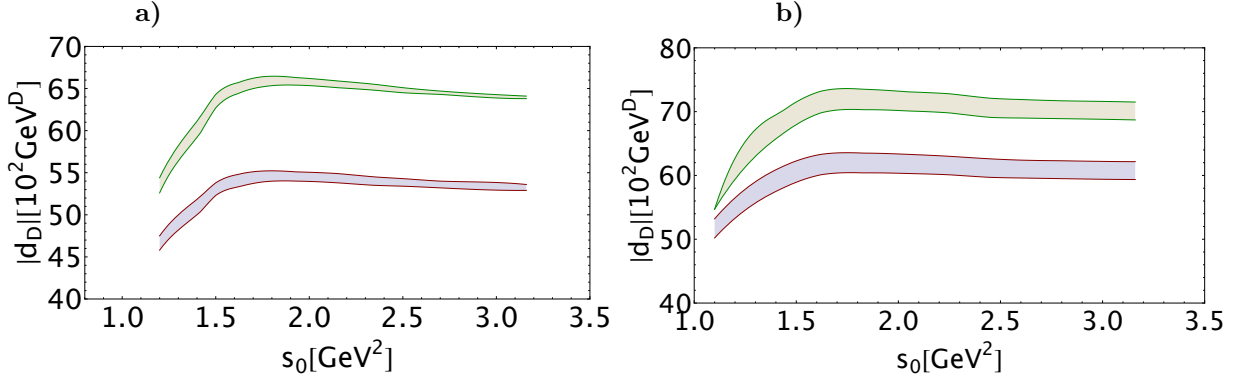


Figure 8: **a)**: $|d_{10,A}|$ (lowest curve) and $|d_{12,A}|$ (highest curve) versus M_0^2 ; **b)**: similar to **a)** but for $|d_{12,A}|$ and $|d_{14,A}|$.

We deduce from $\mathcal{R}_{2,A}$:

$$d_{10,A} = (53.9 \pm 0.7) \times 10^{-2} \text{ GeV}^{10}, \quad d_{12,A} = -(65. \pm 1.) \times 10^{-2} \text{ GeV}^{12} \quad (34)$$

inside the stability region 1.93 GeV^2 to M_τ^2 . We take as a final value of $d_{10,A}$ the mean from $\mathcal{R}_{1,A}$ in Eq. 25 and the one from $\mathcal{R}_{2,A}$ in Eq. 34:

$$d_{10,A} = (53.9 \pm 0.7) \times 10^{-2} \text{ GeV}^{10}. \quad (35)$$

- $d_{2n,A}$ and $d_{2(n+1),A}$ condensates

We do the same procedure as previously for higher dimension condensates $n \geq 6$. The s_0 behaviours of the condensates are shown in Figs. 9, 10. The results are summarized in Table 2.

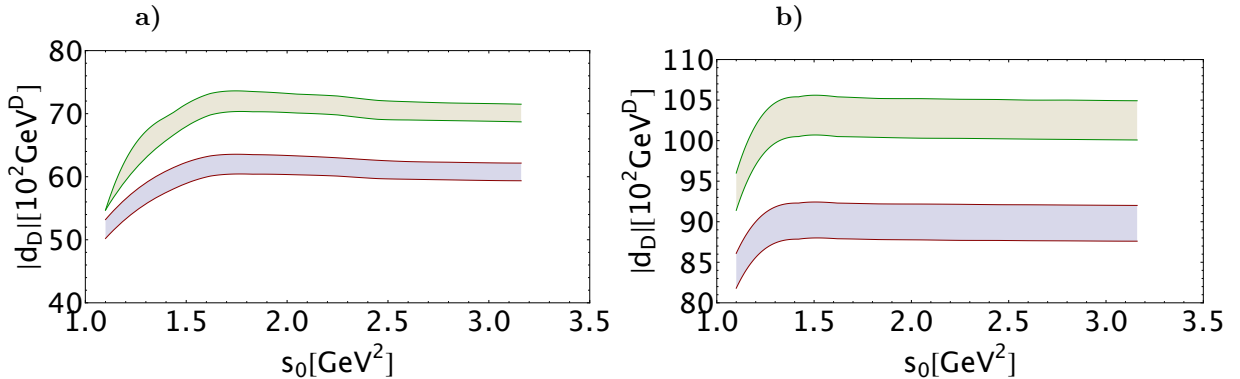


Figure 9: **a)**: $|d_{14,A}|$ (lowest curve) and $|d_{16,A}|$ (highest curve) versus M_0^2 ; **b)**: similar to **a)** but for $|d_{16,A}|$ and $|d_{18,A}|$.

◊ One can notice that the condensates in the A channel has alternate sign.

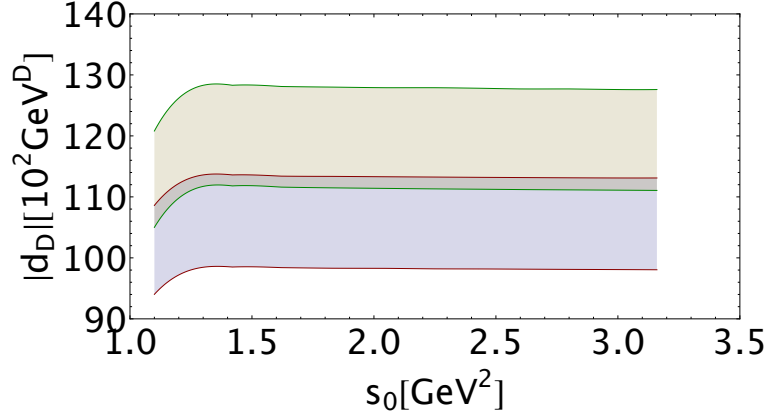


Figure 10: $|d_{18,A}|$ (lowest curve) and $|d_{12,A}|$ (highest curve) versus M_0^2 .

◇ Their size is almost constant and more accurate than previous determinations in the literature. There is not also any sign of an exponential growth. This feature in the Euclidian region does not favour a sizeable duality violation in the time-like region [19].

$d_{6,A}$	$-d_{8,A}$	$d_{10,A}$	$-d_{12,A}$	$d_{14,A}$	$-d_{16,A}$	$d_{18,A}$	$-d_{20,A}$	Refs.
34.4 ± 1.7	51.5 ± 2.1	53.9 ± 0.7	63.3 ± 1.8	77.0 ± 6.0	93.1 ± 4.0	104.3 ± 7.7	119.7 ± 8.2	This work
43.4 ± 13.8	59.2 ± 19.7	63.2 ± 33.6	43.4 ± 31.6					[18]
19.7 ± 1.0	27 ± 1.2							[10]
9.6 ± 3.3	9.0 ± 5.0							[20]

Table 2: Values of the QCD condensates of dimension D in units of 10^{-2} GeV^D from this work and some other estimates.

8. The V–A channel

• The two-point function

Its corresponds to the V–A quark current:

$$J_{V-A}^\mu(x) =: \bar{\psi}_u \gamma^\mu (1 - \gamma_5) \psi_d : . \quad (36)$$

In the chiral limit, the QCD expression of the corresponding two-point function is similar to the one in Eq. 5 where:

$$\begin{aligned}
d_{6,V-A} &= \frac{1}{2} (d_{6,V} + d_{6,A}) = -\frac{1}{2} \left(\frac{4}{7} \right) d_{6,V} \\
&= \frac{512}{27} \pi^3 \rho \alpha_s \langle \bar{\psi} \psi \rangle^2 = (37.5 \pm 1.9) \times 10^{-2} \text{ GeV}^6, \\
d_{8,V-A} &= \frac{1}{2} (d_{8,V} + d_{8,A}) \simeq -(14.5 \pm 2.2) \times 10^{-2} \text{ GeV}^8
\end{aligned} \quad (37)$$

- *Data handling of the spectral function*

The spectral function has been measured by ALEPH [10] which we show in Fig.;11. In order to fit the

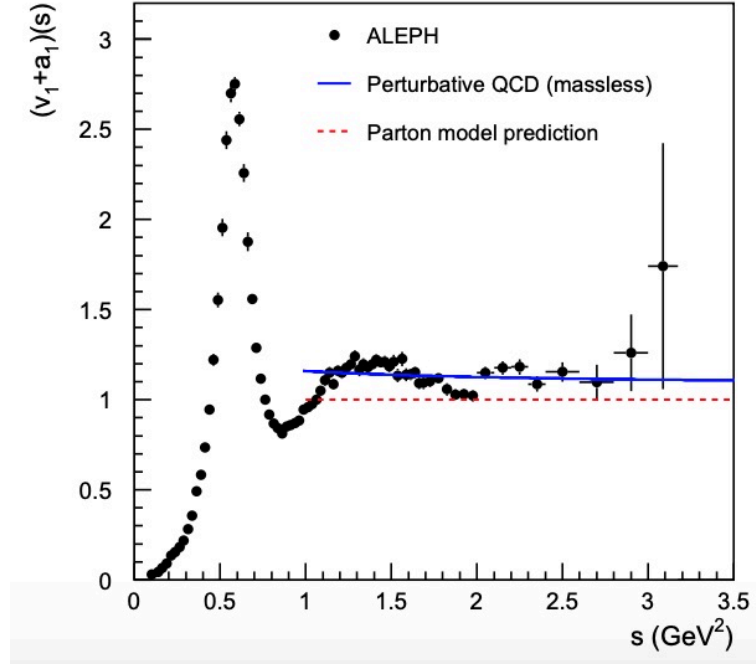


Figure 11: V-A spectral function measured by ALEPH.

data, we proceed like in the case of the axial-vector channel by subdividing the region into 5 subregions :

$$[4m_\pi^2, 0.585], [0.585, 0.85], [0.85, 1.45], [1.45, 1.975], [1.975, M_\tau^2], \quad (38)$$

in units of GeV^2 . We use 3rd order polynomials. The results of the fits are given in Fig. 12.

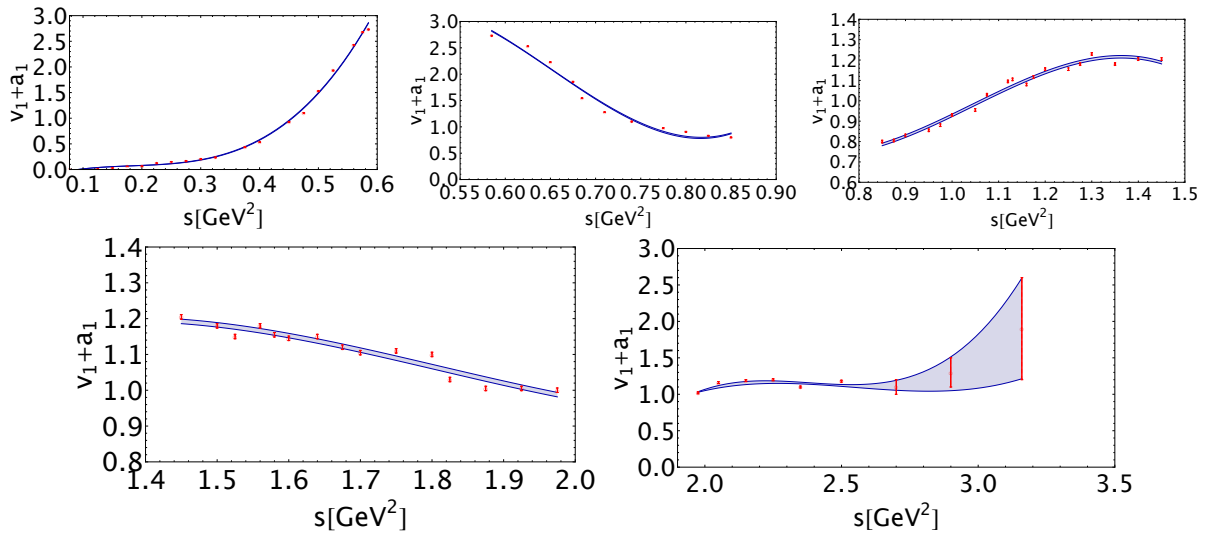


Figure 12: Fit of the data using a 2nd and 3rd order polynomial fits.

- *The lowest BNP moment $\mathcal{R}_{0,V-A}$*

In the chiral limit their expression is similar to the previous ones for the axial-vector current modulo an overall factor 2 and the change into the condensates contributions $d_{D,V-A}$ of dimension D . We show the s_0 behaviour of the moment in Fig.13. For $s_0 = M_\tau^2$, we obtain :

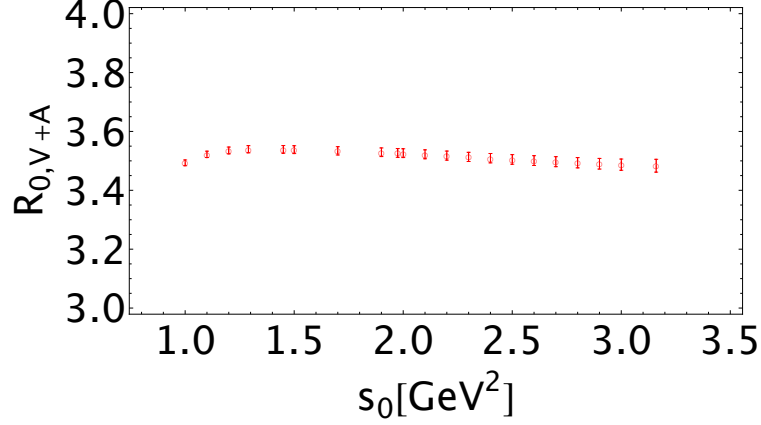


Figure 13: s_0 behaviour of the experimental moment $\mathcal{R}_{0,V-A}$.

$$\mathcal{R}_{0,V-A} = 3.484 \pm 0.022 \quad (39)$$

to be compared with the ALEPH data[10]:

$$\mathcal{R}_{0,V-A}|_{Aleph} = 3.475 \pm 0.011, \quad (40)$$

where our error is larger which may due to the fact that we have separately fitted the upper and lower values of the data.

- *The $d_{6,V-A}$ and $d_{8,V-A}$ condensates*

We shall use the values of the corresponding condensates from the $e^+e^- \rightarrow \text{Hadrons}$ in Ref. [1, 2] and the ones from the axial-vector channel obtained in the previous section. They read:

$$\begin{aligned} d_{6,V-A} &\equiv \frac{1}{2} (d_{6,V} + d_{6,A}) = +(3.6 \pm 0.5) \times 10^{-2} \text{ GeV}^6, \\ d_{8,V-A} &\equiv \frac{1}{2} (d_{8,V} + d_{8,A}) = -(14.5 \pm 2.2) \times 10^{-2} \text{ GeV}^8, \end{aligned} \quad (41)$$

where the error is the largest relative % error from each channel. We note (as can be found in Ref. [4]) that for $\mathcal{R}_{0,V-A}(s_0)$, the contribution of $\langle \alpha_s G^2 \rangle$ is α_s suppressed while the one of $d_{6,V-A}$ is smaller than in the individual V and A channels. Then, we expect that V-A is a *golden channel* for extracting α_s .

- α_s from $\mathcal{R}_{0,V-A}(s_0)$

Using the value of $\langle \alpha_s G^2 \rangle$ in Eq. 12 and the previous values of $d_{6,V-A}$ and $d_{8,V-A}$ in Eq. 41, we extract the value of $\alpha_s(M_\tau)$ as a function of s_0 (see Fig. 14) from $\mathcal{R}_{0,V-A}(s_0)$. We notice a stable result in the

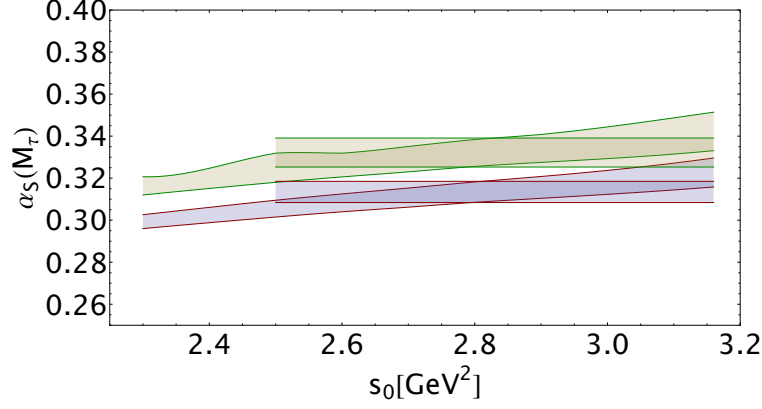


Figure 14: $\alpha_s(M_\tau)$ versus an hypothetical τ -mass squared s_0 . The upper curves corresponds to CI perturbative series and the lower ones to FO. The horizontal lines come from a least-square fit of the data in the optimal region $s_0 \simeq (2.3 \sim 2.9) \text{ GeV}^2$.

region $s_0 \simeq (2.5 \sim 2.6) \text{ GeV}^2$ though not quite convincing. The, we consider as a conservative value the one obtained from a least-square fit of the values inside the region $[2, 5, M_\tau^2]$. The optimal result corresponds $s_0 = 2.8 \text{ GeV}^2$ (see Fig. 14):

$$\begin{aligned} \alpha_s(M_\tau)|_{V-A} &= 0.3135(51)(65) & \longrightarrow & \alpha_s(M_Z)|_{V-A} = 0.1177(10)(3)_{evol} & \text{(FO)} \\ &= 0.3322(69)(43) & \longrightarrow & \alpha_s(M_Z)|_{V-A} = 0.1200(9)(3)_{evol} & \text{(CI).} \end{aligned} \quad (42)$$

The 1st error in $\alpha_s(M_\tau)|_{V-A}$ comes from the fitting procedure. The 2nd one from an estimate of the α_s^5 contribution from Ref. [1]. At this scale the sum of non-perturbative contributions to the moment normalized to the parton model is:

$$\delta_{NP,V-A} \simeq +(2.7 \pm 1.1) \times 10^{-4}, \quad (43)$$

which is completely negligible. One can notice from Fig. 14 that extracting $\alpha_s(M_\tau)|_{V-A}$ at the observed M_τ -mass tends to overestimate its value:

$$\alpha_s(M_\tau)|_{V-A} = 0.3227(69)(65) \quad \text{FO}, \quad 0.3423(92)(43) \quad \text{CI}. \quad (44)$$

- *Comparison with some previous results*

In Table 3, we compare our results with some other determinations [10, 18, 20]³ obtained at the scale $s_0 = M_\tau^2$.

- ◊ There is a quite good agreement for $d_{6,V-A}$ but not for $d_{8,V-A}$ from different determinations.
- ◊ The central values of the condensates given in Table 7 of Ref. [18] using a truncation of the OPE up to $D = 10$ are systematically smaller than the ones in their Table 8 using the OPE up to $D = 12$ though they agree within the errors.

³Some estimates including renormalon within a large β approximation [resp. duality violation] effects can be e.g. found in Refs. [21] [resp. [22]].

$d_{6,V-A}$	$-d_{8,V-A}$	$\alpha_s(M_\tau)$ FO	$\alpha_s(M_\tau)$ CI	s_0 [GeV] ²	Refs.
3.6 ± 0.5	14.5 ± 2.2	0.3135(83)	0.3322(81)	$2.5 \rightarrow M_\tau^2$	This work
3.6 ± 0.5	14.5 ± 2.2	0.3227(95)	0.3423(102)	M_τ^2	This work
$5.1^{+5.5}_{-3.1}$	3.2 ± 2.2	$0.3170^{+0.0100}_{-0.0050}$	$0.3360^{+0.0110}_{-0.0090}$	M_τ^2 ($D \leq 10$)	Table 7 [18]
24^{+24}_{-16}	32^{+25}_{-32}	$0.3290^{+0.0120}_{-0.0110}$	$0.3490^{+0.0160}_{-0.0140}$	M_τ^2 ($D \leq 12$)	Table 8 [18]
2.4 ± 0.8	3.2 ± 0.8	–	0.3410(78)	M_τ^2	[10]
1.5 ± 4.8	3.7 ± 9.0	0.3240(145)	0.3480(212)	M_τ^2	[20]

Table 3: Values of the QCD condensates from \mathcal{R}_{0,e^+e^-} and $\mathcal{R}_{0,A}$ at Fixed Order (FO) PT series and of $\alpha_s(M_\tau)$ for FO and Contour Improved (CI) PT series. The condensates are in units of 10^{-2} GeV^D.

◇ Extracting α_s at M_τ , there is a good agreement among different determinations where the values are slightly higher than the ones from the optimal region given in the first row (see Fig. 14).

9. Mean value of α_s from $e^+e^- \rightarrow$ Hadrons and A, V–A τ -decays

Using the result from $e^+e^- \rightarrow$ Hadrons and from the A and V–A τ -decay channels, we deduce the mean:

$$\begin{aligned}
\alpha_s(M_\tau) &= 0.3140(44) \text{ (FO)} & \longrightarrow & \alpha_s(M_Z) = 1178(6)_{fit(3)_{evol.}}, \\
&= 0.3346(35) \text{ (CI)} & \longrightarrow & \alpha_s(M_Z) = 0.1202(4)_{fit(3)_{evol.}}
\end{aligned} \tag{45}$$

10. Summary

- We have improved the determinations of the QCD condensates in the axial-vector channel using a ratio of LSR and higher BNP-like moments. Our results are summarized in Table 2. We observe alternate signs, an almost constant value of their size. The absence of an exponential behaviour in the Euclidian region may not favour a duality violation in the time-like region [19].

- We have used as inputs the value of $\langle \alpha_s G^2 \rangle$ better determinaed from the heavy quark channels and the ones of the previous condensates $d_{6,A}$ and $d_{8,A}$ to extract $\alpha_s(M_\tau)$ from the lowest BNP-moment $\mathcal{R}_{0,A}(s_0)$. Our conservative result in Eq. 30 is obtained from $s_0 \simeq 2.1$ GeV² to M_τ^2 where we notice from Fig. 7 that extracting $\alpha_s(M_\tau)$ at the observed τ -mass leads to an overestimate of its value.

- We combine the previous values of the $d_{6,A}$ and $d_{8,A}$ with the ones of the $d_{6,V}$ and $d_{8,V}$ from $e^+e^- \rightarrow$ Hadrons [1, 2] into the lowest moment $\mathcal{R}_{0,V-A}(s_0)$ in the V–A channel. Then, we extract the conservative value of $\alpha_s(M_\tau)$ given in Eq. 44 at $s_0 = [2.5 \text{ GeV}^2 \rightarrow M_\tau^2]$. Like in the case of the $e^+e^- \rightarrow$ Hadrons and axial-vector channel, we also notice that extracting $\alpha_s(M_\tau)$ at M_τ leads to an overestimate.

- We have not considered some eventual effects beyond the SVZ-expansion as:

◇ According to Ref. [17], the effect a tachyonic gluon mass [23] for parametrizing phenomenologically the UV renormalon effect is equivalent by duality to the contribution of the uncalculated higher order PT

terms. We assume that these terms are well approximated by the estimate of the α_s^5 term done in the paper using the observation that the coefficients of the calculated PT terms behave as a geometric sum.

◊ The observation that the calculated PT terms behave as a geometric sum and that no signal of alternate sign of these PT terms do not (a priori) favour the motivation of a large β -approximation for the estimate of the UV renormalon.

◊ The non-observation of an exponential behaviour of the non-perturbative condensate effects in the Euclidian region may indicate that Duality Violation in the time-like region [22] may not be sizeable [19].

◊ Instanton effects act as high-dimension operators and their effects have been shown to be negligible in the vector channel [1]. We expect similar features for the A and V–A channels.

Acknowledgement

I thank Toni Pich for a careful reading of the manuscript and the 2nd referee for some constructive comments.

References

- [1] S. Narison, *Nucl. Phys. A* **1046** (2024) 122873, *Nucl. Phys. A* **1050** (2024) 122915 (erratum),
S. Narison, QCD24 (8-12 july 2024, Montpellier-FR), *Nucl. Part. Phys. Proc.* **347** (2024) 105.
- [2] S. Narison, *Nucl. Phys. A* **1039** (2023) 122744;
S. Narison, QCD23 (10-14 july 2023, Montpellier-FR), *Nucl. Part. Phys. Proc.* **343** (2024).
- [3] M.A. Shifman, A.I. Vainshtein, V.I. Zakharov, *Nucl. Phys. B* **147** (1979) 385;
M.A. Shifman, A.I. Vainshtein, V.I. Zakharov, *Nucl. Phys. B* **147** (1979) 448.
- [4] E. Braaten, S. Narison, A. Pich, *Nucl. Phys. B* **373** (1992) 581.
- [5] E. Braaten, *Phys. Rev. Lett.* **60** (1988) 606; E. Braaten, *Phys. Rev. D* **39** (1989) 1458;
S. Narison, A. Pich, *Phys. Lett. B* **211** (1988) 183.
- [6] S.G. Gorishny, A.L. Kataev, S.A. Larin, *Phys. Lett. B* **259** (1991) 144; L.R. Surguladze, M.A. Samuel,
Phys. Rev. Lett. **66** (1991) 560.
- [7] P. A. Baikov, K.G. Chetyrkin, J.H. Kühn, *Phys.Rev.Lett.* **101**(2008) 012002.
- [8] S. Narison, *QCD as a theory of hadrons*, *Cambridge Monogr. Part. Phys. Nucl. Phys. Cosmol.* **17**.
(2004) 1-778 [hep-ph/0205006].
- [9] R.L. Workman et al. (Particle Data Group), *Prog. Theor. Exp. Phys.* **2022** (2022) 083C01.
- [10] The ALEPH collaboration: M. Davier, A. Hoecker, B. Malaescu, C. Yuan, Z. Zhang, *Eur. Phys. J.*
C74 (2014) 2803; <http://aleph.web.lal.in2p3.fr/tau/specfun13.html>.

- [11] S. Narison and E. de Rafael, *Phys. Lett.* **B 103**, (1981) 57.
- [12] J.S. Bell and R.A. Bertlmann, *Nucl. Phys.* **B187**, (1981) 285.
- [13] For a recent review, see e.g. S. Narison, *The Laplace Transform and its Applications*, ed. V. Martinez-Lucaes, Nova Science Pub., New-York - 2024 (arXiv: 2309.00258 [hep-ph]).
- [14] S. Narison, *Int. J. Mod. Phys.* **A33** (2018) no. 10, 185004; Addendum: *Int. J. Mod. Phys.* **A33** (2018) no.10, 1850045.
- [15] S. Narison, *Phys. Lett.* **B693** (2010) 559, erratum *ibid*, **B705** (2011) 544; *ibid*, **B706** (2012) 412; *ibid*, **B707** (2012) 259.
- [16] F. Le Diberder, A. Pich, *Phys. Lett.* **B286** (1992) 147; **B289** (1992) 165.
- [17] S. Narison, V.I. Zakharov, *Phys. Lett.* **B679** (2009) 355.
- [18] A. Pich, A. Rodríguez-Sánchez, *Phys.Rev.* **D94** (2016) 3, 034027; *Mod.Phys.Lett.* **A31** (2016) 30, 1630032; *Nucl. Part. Phys. Proc.* **287-288** (2017) 81.
- [19] M. Shifman, *Nucl. Phys. Proc. Suppl.* **B207-208** (2010) 298; *ibid* arXiv: hep-ph/0009131; B. Blok, M. Shifman, Da-Xin Zhang, *Phys. Rev.* **D 57** (1998) 2691; *Phys. Rev.* **D 59** (1999) 019901 (erratum).
- [20] The OPAL collaboration: K. Ackerstaff et al., *Euro. Phys. J.* **C7** (1999) 571.
- [21] C. Ayala, G. Cvetič, D. Teca, *J.Phys.* **G 50** (2023) n^0 . 4, 045004; M. Beneke, D. Boito, M. Jamin, *JHEP* **01** (2013) 125.
- [22] D. Boito, M. Golterman, K. Maltman, S. Peris, *Phys. Rev.* **D 95** (2017) n^o . 3, 034024
- [23] K.G. Chetyrkin, S. Narison, V. I. Zakharov, *Nucl. Phys.* **B550**(1999) 353.